J Breast Cancer. 2022 Jun;25(3):218-232
https://doi.org/10.4048/jbc.2022.25.e18
pISSN 1738-6756·eISSN 2092-9900

Journal of Breast Cancer JBC

Original Article

Murine Mammary Carcinoma Induces Chronic Systemic Inflammation and Immunosuppression in BALB/c Mice

Dasha Fuentes [1], **Alejandro Cabezas-Cruz** [2], **Circe Mesa** [3], **Tania Carmenate** [3], **Darel Martínez** [3], **Anet Valdés-Zayas** [3], **Enrique Montero** [3], **Rolando Pérez** [3]

[1]National Center for Laboratory Animal Breeding (CENPALAB), Havana, Cuba
[2]Anses, INRAE, Ecole Nationale Vétérinaire D'Alfort, UMR BIPAR, Laboratoire de Santé Animale, Maisons-Alfort, France
[3]Center of Molecular Immunology (CIM), Havana, Cuba

Received: Jul 21, 2021
Revised: Nov 24, 2021
Accepted: Apr 3, 2022
Published online: Apr 26, 2022

Correspondence to
Dasha Fuentes
National Center for Laboratory Animal Breeding (CENPALAB), Calle 3ra Nº 40759 entre 6ta y Carretera Tirabeque, Reparto La Unión, Boyeros, Havana, Cuba.
Email: dasha.fuentes@cenpalab.cu

ORCID iDs
Dasha Fuentes
https://orcid.org/0000-0003-1970-5580
Alejandro Cabezas-Cruz
https://orcid.org/0000-0002-8660-730X
Circe Mesa
https://orcid.org/0000-0001-8342-7779
Tania Carmenate
https://orcid.org/0000-0001-5366-0035
Darel Martínez
https://orcid.org/0000-0002-1603-5801
Anet Valdés-Zayas
https://orcid.org/0000-0002-0849-2172
Enrique Montero
https://orcid.org/0000-0002-7127-6675
Rolando Pérez
https://orcid.org/0000-0002-9498-886X

ABSTRACT

Purpose: The F3II cell line is a highly invasive variant of mammary carcinoma. Although it is frequently used as a model to evaluate the efficacy of immunotherapy, its impact on the immune system remains poorly understood. The main objectives of this study were to evaluate the effects of F3II tumors on the development of chronic inflammation and to characterize tumor-associated immunosuppression.
Methods: Following the experimental implantation of F3II tumors in BALB/c mice, alterations in the liver and spleen anatomy and the numbers of circulating leukocytes, myeloid-derived suppressor cells (MDSCs), and regulatory T cells were measured using hematological techniques, histopathological analysis, and flow cytometry. The capacity of the F3II tumor-bearing mice to reject MB16F10 allogeneic tumor transplantation was also evaluated. In addition, the restoration of immune parameters in tumor-bearing mice was evaluated after standard breast cancer chemotherapy and surgical tumor excision.
Results: F3II tumor implantation increased the levels of chronic inflammatory markers, such as the neutrophil-to-lymphocyte and platelet-to-lymphocyte ratios, and caused myeloid alterations, including extramedullary granulopoiesis and megakaryopoiesis, along with the recruitment of MDSCs to the spleen. Chemotherapy or surgical F3II tumor removal completely rescued the tumor-associated extramedullary granulopoiesis and megakaryopoiesis. Notably, the presence of F3II tumors reduced the capacity of BALB/c mice to reject MB16F10 allogeneic tumor transplantation.
Conclusion: These results support the occurrence of F3II tumor-mediated immune cell dysfunction, which mimics the immune alterations characterized by chronic systemic inflammation and immunosuppression observed in breast cancer in clinical settings. Thus, the F3II tumor model is relevant for evaluating novel breast cancer immunotherapies and combinations in preclinical studies. This model could also be useful for identifying appropriate therapeutic targets and developing proof-of-concept experiments in the future.

Keywords: Immune System; Immunosuppression Therapy; Inflammation; Mice; Neoplasms

Conflict of Interest
The authors declare that they have no competing interests.

Data Availability Statement
The data supporting the findings of this study are available from the corresponding author upon request.

Author Contributions
Conceptualization: Fuentes D, Montero E, Pérez R; Data curation: Fuentes D, Cabezas-Cruz A; Formal analysis: Pérez R; Investigation: Fuentes D, Cabezas-Cruz A, Mesa C, Carmenate T, Martínez D, Valdés-Zayas A; Methodology: Fuentes D, Montero E, Pérez R; Supervision: Montero E; Writing - original draft: Fuentes D; Writing - review & editing: Fuentes D, Cabezas-Cruz A, Carmenate T, Montero E, Pérez R.

INTRODUCTION

The F3II cell line is a highly invasive and hormone-independent variant of mammary carcinoma derived from a spontaneous BALB/c mouse mammary adenocarcinoma clone [1]. F3II cells develop into spindle-cell carcinomas, characterized by extensive local invasion into the muscular and adipose sections of the subcutis, the deepest layer of the skin integument [2]. This tumor is associated with increased angiogenesis and 90%–100% incidence of lung metastases when inoculated subcutaneously into syngeneic mice [1]. Accordingly, the F3II tumor line is thought to be a suitable model for testing the efficacy of anti-invasive, anti-angiogenic, and anti-metastatic agents [1]. Growing F3II subcutaneous tumors secrete the granulocyte macrophage colony-stimulating factor (GM-CSF), which induces massive myelopoiesis in the bone marrow and spleen [3]. Furthermore, the addition of recombinant mouse GM-CSF to F3II cell cultures significantly increases cell growth *in vitro* [3]. These data suggest that ectopic GM-CSF production induces systemic myelopoiesis and immunosuppression, modulating tumor growth and metastasis in vivo [4].

Transplanted F3II tumors present with intratumoral heterogeneity, characterized by a mixture of neoplastic round or cuboidal epithelial cells, sometimes arranged in tubule-like structures, and spindle cells resembling malignant fibroblasts [1]. This phenotype suggests that an epithelial–mesenchymal transition (EMT) occurs, characterized by a cellular plasticity continuum in which different degrees of epithelial and mesenchymal characteristics are observed among the agglomerated cells, with the periphery resembling EMT phenotypes. EMT is a crucial step in the metastatic cascade, tumor progression, and activation of the tumor immune escape program [5,6]. Immune escape, immunoediting, and tumor-induced immunosuppression are mechanisms developed by tumors to prevent destruction by the immune system [7,8]. These mechanisms are associated with reduced patient survival and immunotherapy responses [9,10] and highlight the impact of tumor–host interactions on tumor progression.

Both local and systemic host inflammatory responses play an important role in cancer development and progression, and can influence the patient's response to therapy. Inflammation indices may be used to predict the prognosis of patients with cancer [11,12]. The levels of circulating immune and inflammatory cells, such as neutrophils, monocytes, lymphocytes, and platelets, may contribute to cancer invasion and metastasis [13].

Tumor-induced immunosuppression modulates immune cells via ligand-to-ligand interactions, immunosuppressive cytokine and metabolite secretion, establishment of a hypoxic environment that is unfavorable for effective antitumor immune responses, and recruitment and differentiation of host immunosuppressive cells, such as myeloid-derived suppressor cells (MDSCs) and regulatory T cells (Tregs) [14-16]. Tumors can also suppress immune responses by establishing a niche that excludes immune cells, the so-called "immune desert" phenotype [14].

The development of effective anticancer drugs requires an appropriate mammalian model of tumor growth that recapitulates human disease characteristics to demonstrate measurable effects [17]. The F3II murine tumor model has been used in several preclinical studies to test the efficacy of breast cancer immunotherapy [2,18]. However, only a few studies have explored the effects of F3II tumors on the immune system in tumor-bearing mice [3,19]. Given that F3II tumors produce inflammatory and immunosuppressive effects, this study

aimed to evaluate the impact of this tumor on the development of chronic inflammation and characterize any tumor-associated immunosuppression. We investigated whether F3II tumors modified the number of circulating leukocytes, MDSCs, and Tregs as well as MB16F10 allogeneic tumor transplantation rejection in experimental tumor-bearing BALB/c mice.

METHODS

Ethics statement

All animal studies were conducted according to a protocol approved by the Institutional Animal Care and Use Committee of National Center for Laboratory Animal Breeding (CENPALAB) (permit number 17/17).

Mice and tumor cell lines

Female BALB/c/Cenp and C57Bl/6/Cenp mice at 6–10 weeks of age were obtained from the National Center for Laboratory Animal Breeding (CENPALAB, Havana, Cuba) and maintained in standard housing (Tecniplast, Varese, Italy). Autoclaved EAO 1004 food (CENPALAB) and water were provided *ad libitum*. The room temperature (20°C–23°C), humidity (65% ± 10%), and photoperiod cycles (12 hours per day) were automatically controlled. The animals were monitored twice daily by an experienced technician for any abnormal reactions, health problems, or complications.

Stocks of F3II tumor and MB16F10 melanoma cells were maintained in a minimal essential medium (MEM 41500; Gibco BRL, Grand Island, USA) supplemented with 10% fetal bovine serum (FBS; Gibco BRL), 2 mM glutamine (Gibco BRL), 80 mg/mL of gentamycin (Gibco BRL), and 20 mg/mL of tetracycline (Gibco BRL) in monolayer cultures. Cell viability was assessed using the trypan blue exclusion assay. For inoculation, 1×10^6 F3II cells or 2.5×10^6 MB16F10 cells were diluted in 1 mL of phosphate-buffered saline (PBS; CENPALAB).

F3II tumor inoculation and allogeneic MB16F10 tumor rejection protocol

BALB/c mice were subcutaneously inoculated with 200 µL of F3II tumor cells (2×10^5 cells/mouse) in the right flank. Tumor implantation was monitored by gentle palpation of the tumor inoculation site every alternate day. After inoculation, the tumor size was measured twice a week using a caliper (Mitutoyo, Kawasaki, Japan). The volume of each individual tumor was computed using the formula: $V = \pi ab^2/6$, where a is the major tumor diameter and b is the minor diameter. Animals were sacrificed for ethical reasons if the tumor reached 2000 mm^3 in size or became ulcerated. A group of non-inoculated BALB/c mice (hereafter referred to as "naïve mice") was used as the control.

To evaluate the effect of F3II tumors on the capacity of mice to reject an allogeneic tumor, BALB/c mice (n = 10/group) were injected with F3II cells, and 21 days later, with 200 µL of the allogeneic melanoma cell line MB16F10 (5×10^5 cells/mouse) in the left flank. MB16F10 melanoma cells alone were inoculated into either C57BL/6 mice that cannot naturally reject MB16F10 tumors or into BALB/c mice that were considered as positive and negative tumor controls, respectively. Melanoma tumor size was measured seven days after inoculation and twice a week thereafter.

https://doi.org/10.4048/jbc.2022.25.e18

Blood sample collection and measurement of hematologic parameters

Blood samples were obtained from the maxillary sinuses of naïve and tumor-bearing BALB/c mice 35 days after F3II tumor inoculation. Samples were mixed with ethylenediaminetetraacetic acid (EDTA), and the differential white blood cell (neutrophils, lymphocytes, monocytes, eosinophils, and basophiles) and platelet counts were measured using a hematological automatic analyzer (Micros ABX; Roche Diagnostic Systems, Mannheim, Germany). The neutrophil-to-lymphocyte ratio (NLR) and platelet-to-lymphocyte ratio (PLR) were calculated by dividing the absolute neutrophil or platelet count by absolute lymphocyte count.

Cytostatics and chemotherapy

The cytostatics, doxorubicin (Lemery, Mexico City Mexico) and cyclophosphamide (Lemery), were diluted in PBS. The same standard high chemotherapeutic doses used for human breast cancer (60 mg/m^2 doxorubicin and 600 mg/m^2 cyclophosphamide) were used in BALB/c mice seven days after F3II tumor inoculation. The animals were separated into different groups (n = 10 mice/group) and treated intravenously with doxorubicin and cyclophosphamide. The negative control group was administered PBS via the same route. The time to appearance of local tumors and tumor size were measured as described above.

F3II tumor removal by surgery

Surgical excision of the primary F3II tumors was performed 35 days after tumor inoculation in a group of mice (n = 10). Before surgery, the mice were anesthetized and the tumors were resected with sterilized instruments. All mice survived the surgery. No tumor recurrence was detected at the site of surgical excision.

Organ collection and pathological analysis

Euthanasia and complete necropsy of tumor-bearing and naïve BALB/c mice were performed 35 days after F3II cell inoculation and 30 days after F3II tumor removal via surgery. The spleens, livers, lungs, kidneys, hearts, brains, and tumors from the animals were dissected and weighed after euthanasia. The ratio of organ weight to body weight without tumors was calculated. Representative organ samples were collected and preserved in 10% neutral phosphate-buffered formalin (ERCROS, Barcelone, Spain). Sections of the preserved tissues were processed using standard histological procedures. Briefly, paraffin-embedded tissues were sectioned, stained with hematoxylin (Merck, Darmstadt, Germany) and eosin (Merck), and examined by a veterinary pathologist using a light microscope (Olympus, Tokyo, Japan). To investigate the presence of spontaneous metastases, the lungs were removed and fixed in Bouin's solution (Merck) (5% acetic acid, 9% formaldehyde, and 0.9% picric acid) for 24 hours, and two independent observers determined the number of surface lung nodules using a dissecting stereo microscope (Olympus).

Flow cytometry and cell analysis

For flow cytometry, cell suspensions from the spleen were prepared according to standard protocols. Briefly, spleens from BALB/c mice were passed through a cell strainer with a 30 μm pore size using a syringe plunger. Red blood cells were lysed with a lysis solution (155 mM NH_4Cl, 12 mM $NaHCO_3$, and 0.1 mM EDTA). Cells were individually incubated with the antibodies CD11b-FITC (Caltag Laboratories, Burlingame, USA), Gr1-FITC (BD Pharmingen, San Diego, USA), or CD4-FITC (BD Pharmingen) in fluorescence-activated cell sorting (FACS) buffer (PBS containing 2% FCS and 0.1% NaN_3). After incubation in an ice bath for 30 minutes, the cells were washed with the FACS buffer, resuspended in the same buffer, and

https://doi.org/10.4048/jbc.2022.25.e18

analyzed for cells quantification. For Treg determination, CD4-positive cells were stained with anti Foxp3-PE Mab using Foxp3 staining buffer (eBioscience, San Diego, USA), following the manufacturer's recommendations. Data were collected on a FACScan flow cytometer (Becton Dickinson, Franklin Lakes, USA) and analyzed using the FlowJo software (Tree Star Inc., Ashland, USA). All staining profiles were based on live-gated cells, as determined by forward and side scatter properties.

Major histocompatibility complex (MHC) expression and cytokine production by F3II cells

Monolayer F3II cell cultures were treated with trypsin-EDTA (Gibco BRL) for 5 minutes at 37°C.After two washes with MEM 41500 (Gibco BRL) containing 10% FBS (Gibco BRL), the cells were counted using a Neubauer hemocytometer (Merck). A total of 2×10^5 cells in 1 mL of PBS containing 1% bovine serum albumin were added to each well of a 96-well round (U) bottomplate. MHC I and II expression levels were determined after incubating the cells for 20 min on ice with anti-H-2K^{d}FITC and anti-IA/IE PE antibodies (BD Biosciences, Franklin Lakes, USA). Cytokine production was detected using intracellular staining. Cells were fixed and permeabilized with BD Cytofix/Cytoperm Buffers (BD Biosciences) and incubated with anti-interleukin (IL)-10, anti-IL-1β, anti-transforming growth factor (TGF)-β, anti-IL-6, or anti-tumor necrosis factor (TNF)-α antibodies. All antibodies were purchased from BD Biosciences. For each activation marker, an autofluorescence threshold was established by staining the control cells with the corresponding isotype controls. Staining was detected using a Gallios analyzer flow cytometer (Beckman Coulter, Brea, USA) and analyzed using the Kaluza 1.2 software (Beckman Coulter) for all immunofluorescent flow cytometry investigations.

Statistical analyses

All statistical analyses were performed using the SPSS Data Analysis Program (version 10.0; SPSS, Inc., Chicago, USA). Statistical evaluation was performed using a complete randomized analysis of variance (ANOVA) design with significance assessed at $p < 0.05$ (ANOVA). When data did not have a normal distribution, the Kruskal-Wallis test and two-tailed Mann-Whitney test were used. The effect of treatment on primary F3II tumor incidence was compared using the χ^2 test. Each experiment was repeated at least twice.

RESULTS

F3II cells express surface MHC I and produce the pro-inflammatory cytokine IL-6 in vitro

The expression levels of MHC molecules on the surface of F3II tumor cells were determined using flow cytometry. A high percentage (86.17%) of MHC I H-2Kd-positive cells were observed; however, no staining for MHC II I-A/I-E was detected (**Figure 1A**). The extent of cytokine secretion by F3II cells was assessed *in vitro*. Intracellular staining demonstrated that the tumor cells secreted a significant quantity of the pro-inflammatory cytokine, IL-6 (34.53%). In contrast, low expression levels of IL-1β (5.40%), TNF-α (5.17%), and IL-10 (4.61%) were observed (**Figure 1B**).

F3II primary tumors, but not lung metastases, recruit host immune cells and fibroblasts to the periphery of the tumor

Clinical and pathological examination indicated that F3II primary tumors grew by filling the subcutis and were highly locally invasive into neighboring tissues, such as the muscle and

https://doi.org/10.4048/jbc.2022.25.e18

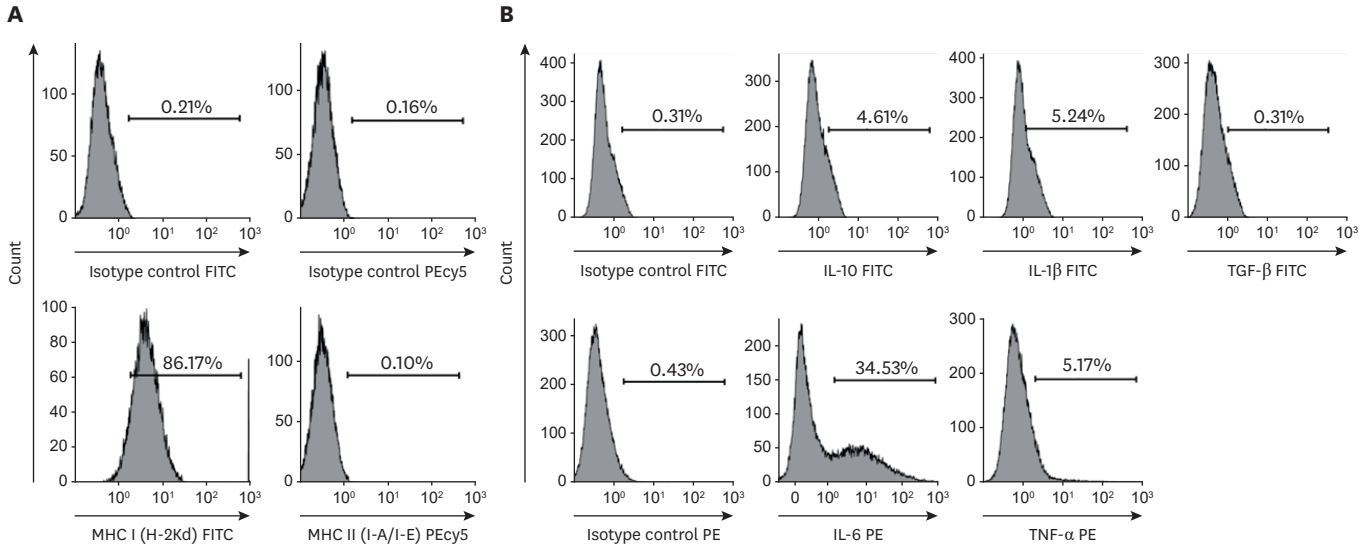

Figure 1. F3II tumor cell line expresses the MHC I (H-2Kd) and produces IL-6. Cell staining measurements. (A) Expression levels of MHC I (H-2Kd) and MHC II (I-A/I-E) molecules on the surface of F3II cells. (B) Intracellular cytokine staining for IL-10, IL-1β, TGF-β, IL-6, and TNF-α.
FITC = fluorescein isothiocyanate; MHC = major histocompatibility complex; IL = interleukin; TGF = transforming growth factor; TNF = tumor necrosis factor.

dermis. A high incidence of pulmonary metastases was observed, and extrapulmonary tumor colonies were not found in any mouse.

Histological analysis of the primary tumors demonstrated a compact mass with little connective tissue stroma, characterized by a mixture of neoplastic round or cuboidal epithelial cells and spindle-shaped cells without lymphocytic intratumoral infiltration (**Figure 2A**). Microvessel density was also increased.

Few neutrophils or lymphocytes were observed within the scant tumor connective stroma; however, macrophages and fibroblasts were particularly abundant (**Figure 2B**). Tumor samples showed high local invasiveness into the muscle and adipose layers of the subcutis and dermis (**Figure 2C**), sometimes reaching the abdominal wall and/or surrounding the last rib and spine. Numerous tumor cells, neutrophils, and leukocytes were detected within the blood vessels, supporting hematogenous tumor cell dissemination mechanisms (**Figure 2D**).

Histological examination of the lungs from tumor-bearing mice revealed metastatic nodules identified as poorly differentiated adenocarcinomas with variable degrees of cellular anaplasia. In several instances, metastatic nodules presented with a sarcomatoid aspect. Some nodules were perivascular, suggesting a hematogenous spread (**Figure 2E**). Subpleural, peribronchial, and alveolar metastases were also observed (**Figure 2F-H**), suggesting that the lymphatic spread of tumor cells could have occurred. In all cases, metastatic nodules exhibited irregular borders, without connective stroma or inflammatory cells at the periphery or inside the tumor.

F3II tumors induce myeloid changes that are reversible with chemotherapy or surgery

At the end of the experiment and 35 days after tumor inoculation, F3II tumor-bearing mice presented with severe neutrophilia ($p < 0.0001$, Mann-Whitney test) in comparison to naïve animals (**Figure 3A**), without alterations to the absolute numbers of circulating lymphocytes ($p > 0.05$, Mann-Whitney test, **Figure 3B**). Consequently, an increase in NLR ($p < 0.0001$,

https://doi.org/10.4048/jbc.2022.25.e18

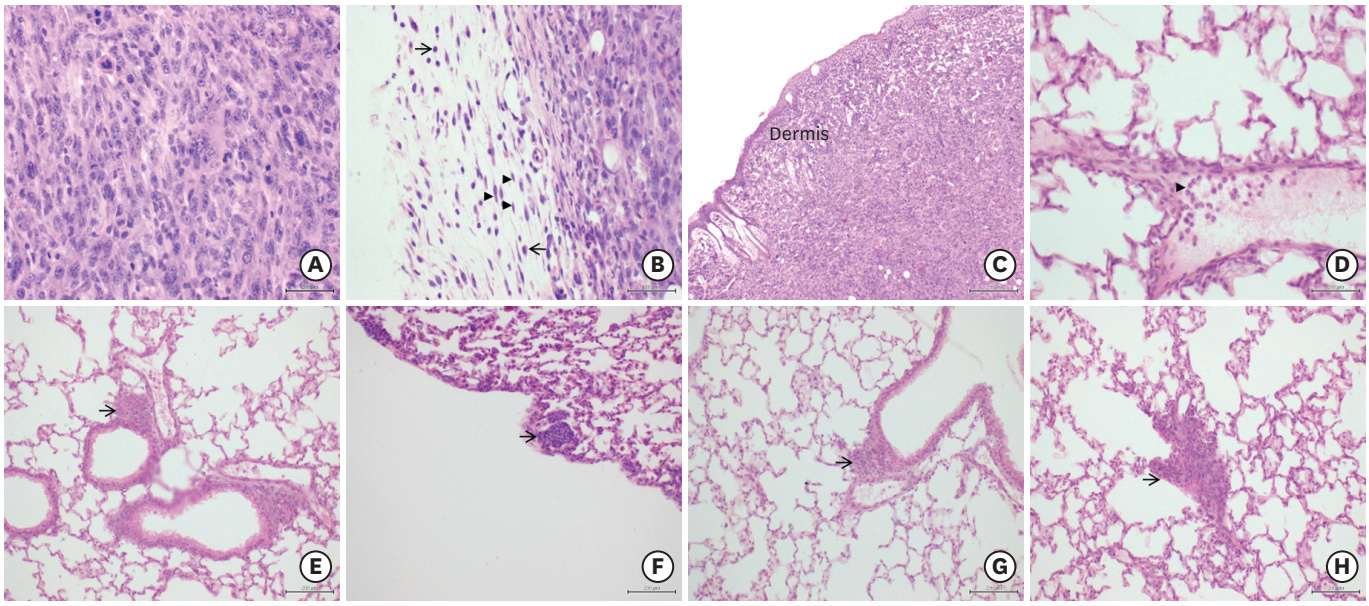

Figure 2. F3II primary tumors recruit host immune cells and fibroblasts to the tumor periphery. Spindle cell carcinomas in BALB/c mice bearing F3II tumors, where abundant macrophages and some neutrophils and lymphocytes were detected near the primary tumor. (A) Histological study demonstrating a mixture of neoplastic round or cuboidal epithelial cells and spindle cells resembling malignant fibroblasts. H&E stain, 400× magnification. Scale bar, 100 μm (B) Scant tumoral connective stroma with abundant macrophages (↑) and fibroblasts (arrowhead). H&E stain, 400× magnification. Scale bar, 100 μm. (C) High degree of invasiveness into the subcutis and dermis. H&E stain, 100× magnification. (D) Numerous neutrophils/leukocytes (arrowhead) were detected inside the blood vessels. H&E stain, 1,000× magnification. (E) Perivascular metastatic lung nodules (↑). H&E stain, 100× magnification. (F) Subpleural metastatic lung nodules (↑). H&E stain, 100× magnification. (G) Peribronchial metastaticlung nodules (↑). H&E stain, 100× magnification. (H) Metastaticlung nodules located in the alveolar wall (↑). H&E stain, 100× magnification. Scale bar, 200 μm.
H&E = hematoxylin and eosin.

Mann-Whitney test) was confirmed (**Figure 3C**). A significant increase in platelet count was also observed ($p < 0.0001$, Mann-Whitney test, **Figure 3D**), which was associated with increased PLR ($p < 0.0001$, Mann-Whitney test, **Figure 3E**).

Tumor presence was not associated with significant changes in the weights of the kidneys, hearts, lungs, and brains of the animals ($p > 0.05$, Mann-Whitney test). However, a significant increase in the liver and spleen weights ($p < 0.05$, Mann-Whitney test) was found in all mice with F3II tumors compared with naïve mice (**Figure 4A**). A positive correlation between the tumor weight and spleen weight ($r^2 = 0.88$, Spearman r = 0.9, $p = 0.015$, **Figure 4B**) and liver weight ($r^2 = 0.88$, Spearman $r = 0.9$, $p = 0.005$, **Figure 4C**) was identified.

Spleen and hepatic histological examinations showed extramedullary granulopoiesis and megakaryopoiesis in mice that received subcutaneous tumor cell injections. The extramedullary processes were characterized by an increased number of immature granulocytic precursors and megakaryocytic hyperplasia in the red pulp of the spleen (**Figure 4D**) and hepatic sinusoids around the central veins or portal vessels. Morphometric assessment of the spleen demonstrated abundant megakaryocytes per field in F3II tumor-bearing mice, whereas in naïve animals, few megakaryocytes per field were observed (**Figure 4E**).

Chemotherapy treatment of F3II tumor-bearing mice significantly reduced the tumor growth (**Figure 4F**) and size ($p < 0.0001$, Mann-Whitney test, **Figure 4G**). In naïve animals, the treatment did not induce any significant variations in organ weight. Likewise, chemotherapy reversed the increase in liver and spleen weights found in F3II tumor-bearing mice ($p < 0.05$, Kruskal-Wallis and Tukey's multiple comparison tests, **Figure 4H**).

https://doi.org/10.4048/jbc.2022.25.e18

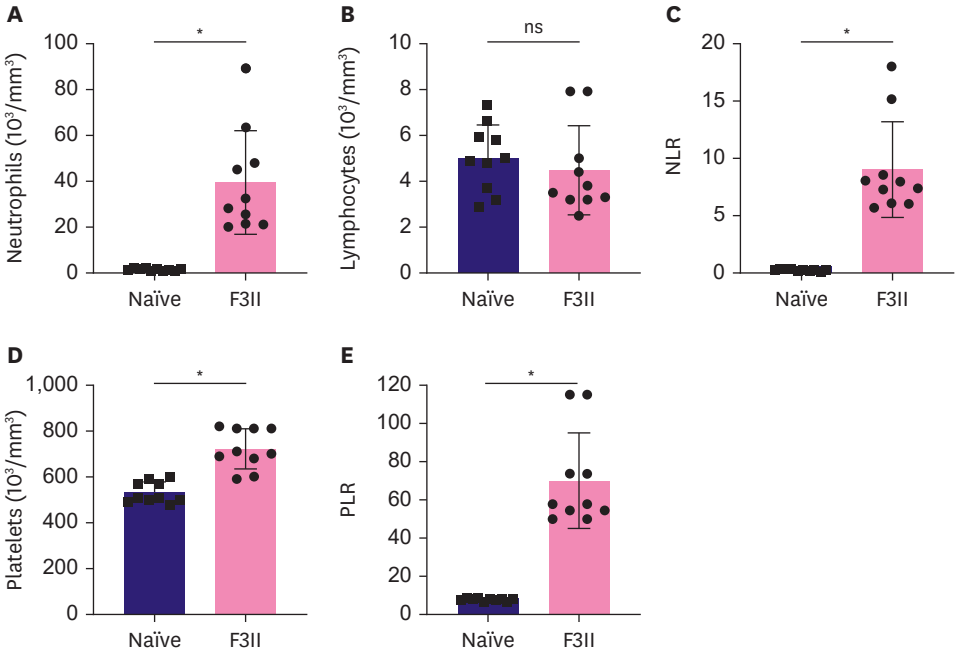

Figure 3. F3II tumors induce severe neutrophilia and significantly increase the number of platelets. F3II tumors induced significant increases in the numbers of neutrophils and platelets, without any change in the number of lymphocytes, resulting in an increase in the NLR and PLR. (A) Neutrophil count (10^3/mm^3). (B) Lymphocyte count (10^3/mm^3). (C) NLR. (D) Platelet count (10^3/mm^3). (E) PLR. Results shown represent the means and SE values. Data were compared using non-parametric Mann-Whitney test (NS; $p > 0.05$). Data from two experiments, n = 10. NLR = neutrophil-to-lymphocyte ratio; PLR = platelet-to-lymphocyte ratio; NS = not significant.
*$p < 0.0001$.

To determine the effects of surgical treatment on F3II tumor-induced myeloid alterations, mice were anesthetized 35 days after tumor cell injection and tumors were resected in half of the tumor-bearing mice. Thirty days after surgical treatment, all animals were sacrificed. Hepatomegaly and splenomegaly were significantly reduced in surgically treated mice compared to non-surgically treated tumor-bearing mice, with values comparable to tumor-free mice ($p < 0.05$, Kruskal-Wallis and Tukey's multiple comparison tests, **Figure 4I**), and spontaneous lung metastases did not increase ($p = 0.4716$, Mann-Whitney test, **Figure 4J**).

Microscopic examination of the spleen and liver showed significant reduction in extramedullary granulopoiesis and megakaryopoiesis in mice treated with either chemotherapy or surgery. These mice had a moderate hematopoietic response, characterized by few granulocytic foci and reduced numbers of megakaryocytes in both organs, similar to that in naïve mice.

F3II tumors were associated with increased number of MDSCs, but not Tregs, in the spleen of BALB/c mice

Spleen cells from naïve BALB/c or F3II tumor-bearing mice were analyzed using flow cytometry to detect CD11b$^+$/Gr1$^+$ and CD4$^+$/FoxP3$^+$Tregs. As shown in **Figure 5A**, splenic CD11b$^+$/Gr1$^+$MDSCs, which are associated with a suppressor phenotype, were present in low numbers in the spleens of tumor-free mice. In contrast, tumor-bearing mice showed a marked increase in this splenic population ($p = 0.01$, Mann-Whitney test), while no differences in Treg cell numbers were detected (**Figure 5B**) compared to the naïve animals ($p = 0.54$, Mann-Whitney test).

https://doi.org/10.4048/jbc.2022.25.e18

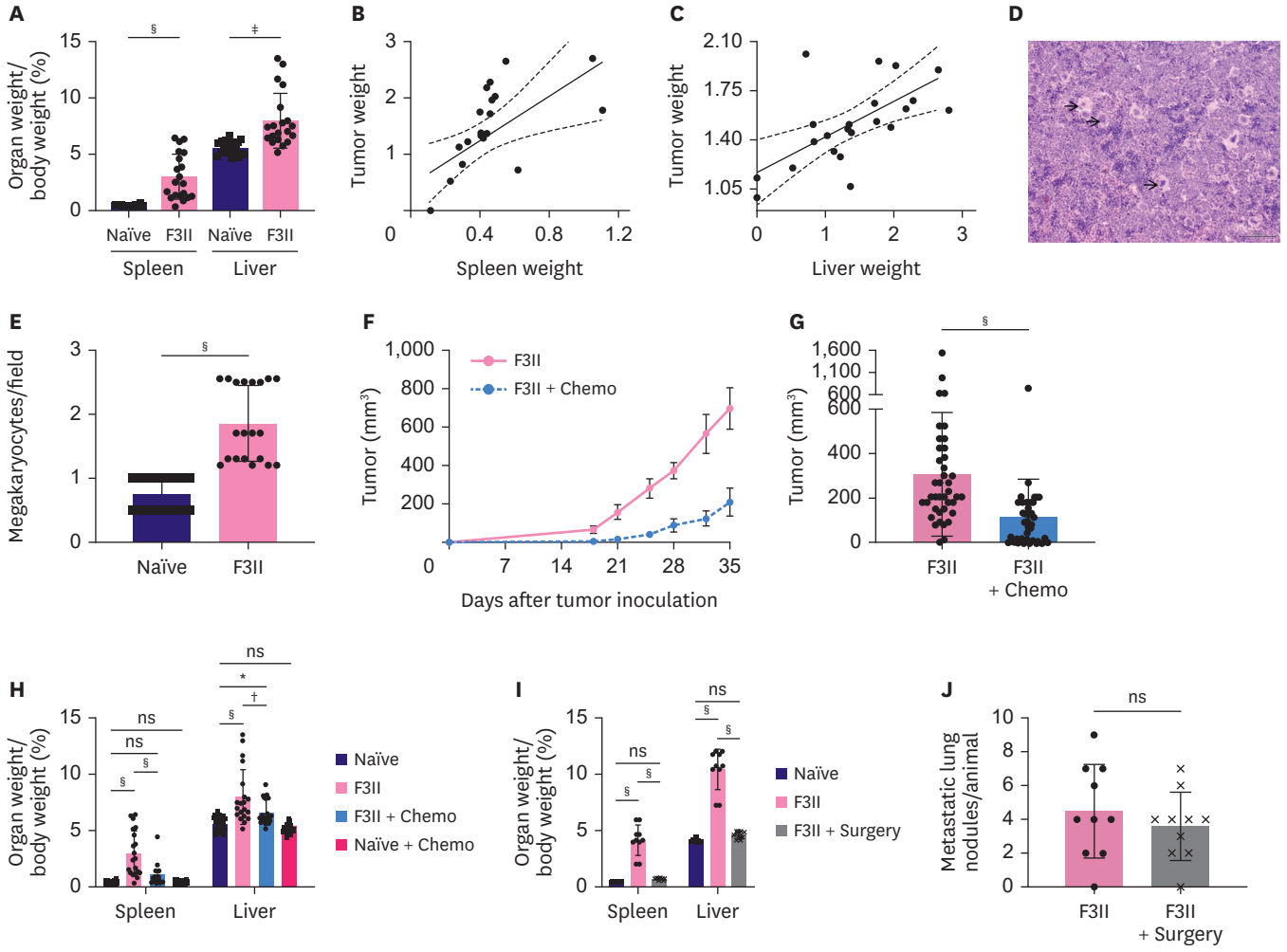

Figure 4. F3II tumors induce massive extramedullary granulopoiesis and megakaryopoiesis, which is reversed by chemotherapy and surgery. F3II tumors induced significant increases in spleen and liver weights associated with massive extramedullary granulopoiesis and megakaryopoiesis compared to the control group, which can be reversed by chemotherapy and surgery. (A) Spleen and liver weights. (B) Correlation between tumor and spleen weights (p = 0.015, Spearman r = 0.9). (C) Correlation between tumor and liver weights (p = 0.005, Spearman r = 0.9). (D) Spleen showing abundant megakaryocytes (↑) and myeloblast foci in red pulp. H&E stain,100× magnification. (E) The number of megakaryocytes was significantly increased in the tumor-bearing mice compared with the control group. (F) High-dose chemotherapy with 600 mg/m² of cyclophosphamide and 60 mg/m² of doxorubicin (Chemo) provokes a significant reduction in tumor growth. (G) Significant reduction in tumor size 35 days after tumor inoculation provoked by high-dose chemotherapy with 600 mg/m² of cyclophosphamide and 60 mg/m² of doxorubicin (Chemo). (H) Spleen and liver weights 35 days after tumor inoculation and chemotherapy. (I) Spleen and liver weights 35 days after tumor inoculation and 30 days after the surgical excision of tumor. (J) Metastatic nodules in the lungs. Results shown represent the means and standard error values. Data were compared using non-parametric Mann-Whitney test or Kruskal-Wallis and Tukey's multiple comparison tests (NS; $p > 0.05$). Data from two experiments, n = 10. Scale bar, 200 μm.
NS = not significant.
*$p < 0.05$, †$p < 0.01$, ‡$p < 0.001$, §$p < 0.0001$.

Rejection of MB16F10 allogeneic tumors is impaired in animals with F3II tumors

To evaluate the effects of syngeneic F3II tumors on the murine immune system, we studied whether the presence of F3II tumors affected the engraftment of allogeneic MB16F10 tumors in BALB/c mice. As shown in **Figure 6A**, all C57Bl/6 mice developed MB16F10 tumors, whereas all naïve BALB/c mice rejected tumor implantation. In contrast, 50% of F3II tumor-bearing BALB/c mice were unable to reject MB16F10 allogeneic tumor implantation. This tumor grows as black spots on the skin; histopathological examination revealed the presence of oval or round cells with small nuclei and numerous melanin-containing cells of variable size and shape, with the majority being round or irregularly polygonal in shape (**Figure 6B**).

https://doi.org/10.4048/jbc.2022.25.e18

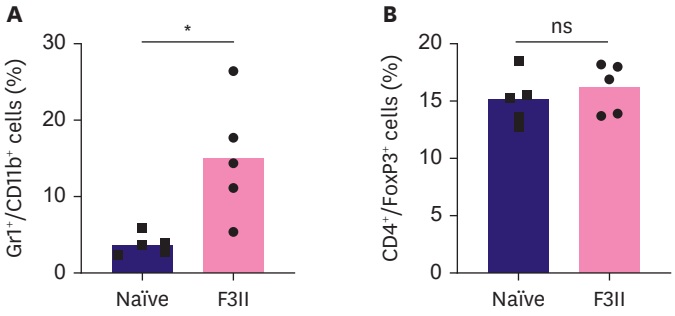

Figure 5. Extramedullary granulopoiesis in mice bearing F3II tumors is related to the recruitment of myeloid-derived suppressor cells in the spleen. (A) The number of splenic GR1$^+$/CD11b$^+$ cells was increased in F3II tumor-bearing mice compared to the negative controls. (B) No differences were found in CD4$^+$/FoxP3$^+$ splenic cell numbers between F3II tumor-bearing mice and the negative controls. Results shown represent the means and standard error values. Data were compared using non-parametric Mann-Whitney test (NS; $p > 0.05$). The values represent the mean of two different experiments, n = 5.
NS = not significant.
*$p < 0.05$.

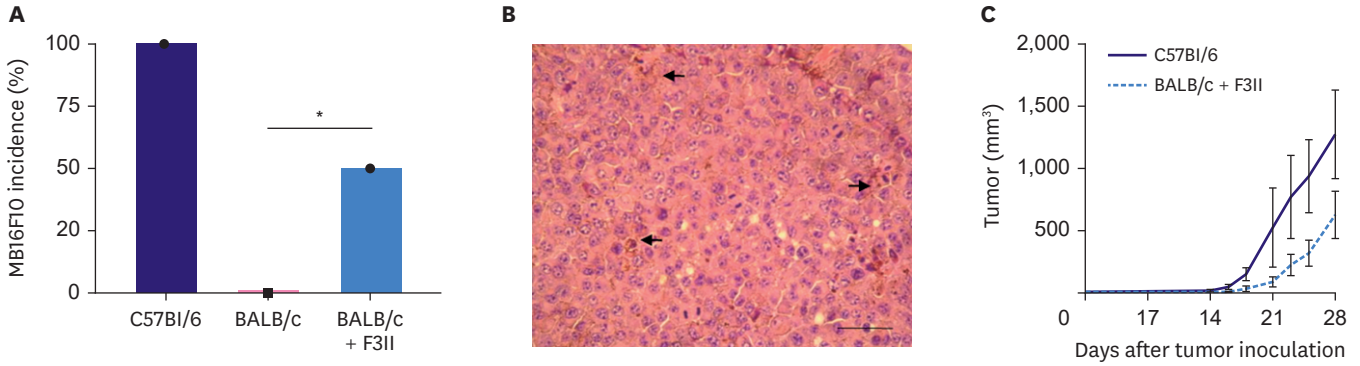

Figure 6. Syngeneic F3II tumors abrogate allogeneic MB16F10 tumor rejection in BALB/c mice. (A) Mice inoculated with F3II tumors were challenged with MB16F10 tumors. The bars indicate the percentage of mice developing tumors. Data were compared using one-tailed Pearson's χ^2 test. The values represent the mean of two different experiments, n = 10. (B) Histological study of MB16F10 allogeneic tumor in BALB/c mice, demonstrating oval or round cells with small nuclei and numerous melanin-containing cells (↑). H&E stain, 400× magnification. Scale bar, 100 μm. (C) Growth kinetics of MB16F10 allogeneic tumor in BALB/c and C57Bl/6 mice. Results shown represent the means and standard error values. Data were compared using non-parametric Mann-Whitney test. The values represent the mean of two different experiments, n = 10.
*$p < 0.05$.

The growth kinetics of the tumor were slightly slower in BALB/c mice than in C57Bl/6 mice (**Figure 6C**), although no significant differences were detected. This result demonstrates that MB16F10 allogeneic tumor rejection is impaired in mice with F3II tumors.

DISCUSSION

Tumors utilize various mechanisms to evade host immunological surveillance or counterattack the immune response to facilitate their progression [20]. During their growth, tumors can downregulate antitumor immune responses via multiple mechanisms capable of interfering with various stages of immune cell development, differentiation, migration, and cytotoxicity [21].

One interesting result of our study was that tumor cells secreted large amounts of MHC I, which is a hallmark of malignant transformation and tumor immune escape. Some authors have reported MHCI downregulation in cancer cells and suggested that this could be an evolutionary mechanism to evade the immune system, where by malignant cells develop

https://doi.org/10.4048/jbc.2022.25.e18

low immunogenic phenotypes with altered antigen-presentation ability [22]. In our case, tumor cells expressing large amounts of MHC I, which were not recognized by cytotoxic T lymphocytes, could be associated with an immunosuppressive process.

In our study, lymphocytes did not infiltrate the primary tumors, and only a few lymphocytes were detected around the tumor periphery along with abundant macrophages and fibroblasts. This observation corroborates previous F3II tumor studies and suggests the presence of a T cell exclusion phenomenon [19], where stromal cells from the tumor microenvironment somehow exclude T cells from their vicinity, resulting in immune evasion and suppression [8,23]. This type of immunological “exclusion” has been described in human tumors and is represented by an increased influence of immunosuppressive reactive stroma, MDSCs, and angiogenesis, all of which prevent T cells from infiltrating tumors or suppress T cell activation within the tumor milieu [24].

In contrast, pulmonary metastases did not contain connective stroma or peripheral inflammatory cells, confirming the heterogeneity between the primary and metastatic tumor sites. Further studies are required to better understand the immunosuppressive role of the tumor microenvironment and the mechanisms by which it excludes T cells [8].

Liver and spleen enlargement related to F3II tumor progression are associated with extramedullary myelopoiesis and GM-CSF production [3]. In the present study, we corroborate these findings and provide evidence that the presence of carcinoma is also related to marked neutrophilia and thrombocytosis linked to a decreased lymphocyte-mediated immune response to malignancy.

Cancer-induced inflammatory responses play dual roles in tumor development throughout various stages, including cancer initiation, promotion, malignant conversion, invasion, and metastasis [25]. Elevated neutrophil and platelet counts are associated with the production of growth factors and cytokines, such as TNF, IL-1β, IL-6, IL-8, TGF-β, as well as the proangiogenic factor, vascular endothelial growth factor (VEGF), which can accelerate tumor development and initiate EMT in cancer cells [26,27].

Increased NLR, the ratio of absolute neutrophils to absolute lymphocytes, is observed in the peripheral blood of patients with cancer, where a higher NLR is associated with a more advanced or aggressive stage of the disease [28-30]. Nevertheless, Fridlender et al. [31] provided evidence for neutrophil polarization, characterized by the existence of N1 (antitumor) and N2 (protumor) tumor-associated neutrophils, analogous to M1 and M2 macrophage polarization. Thus, neutrophils exhibit remarkable plasticity, as demonstrated by their ability to polarize into functionally distinct phenotypes that either support or inhibit tumor growth, depending on signals from the tumor microenvironment [32]. The functional capacity of increased circulating neutrophils in F3II-bearing mice was not evaluated in the present study, which is a limitation of this study. The specific role of neutrophils in murine F3II mammary carcinoma requires further study, although most studies indicate that myeloid immune cells play dominant tumor-promoting and immunosuppressive roles in the tumor microenvironment [13,33,34].

Our results demonstrate that F3II tumor cells secrete several cancer-associated inflammatory components, namely IL-6, IL-1β, IL-10, and TNF-α, which stimulate thrombocytosis and granulopoiesis, generating a "positive feedback loop," in which malignant cells produce

https://doi.org/10.4048/jbc.2022.25.e18

cytokines, thereby inducing platelet and neutrophil production and activation. Furthermore, greater numbers of platelets and neutrophils promote tumor growth and distant metastasis [26,35]. Exposing carcinoma cells to TNF-α, IL-6, IL-10, and IL-8 can directly induce EMT-related transcription factors and favor a mesenchymal phenotype *in vitro* [36]. The presence of EMT-like features can be associated with inflammation and upregulation of immunosuppressive signals/targets in human carcinomas [5].

Tumor cells have evolved multiple sophisticated mechanisms to escape immune surveillance, one of which is establishing a suppressive microenvironment by recruiting cells with immuno-suppressive activity, such as Tregs and MDSCs [14,15,37]. Our results demonstrated an accumulation of MDSCs in the spleens of tumor-bearing mice. Thus, F3II tumors alter normal hematopoiesis and recruit MDSCs to the spleen. As MDSCs inhibit the adaptive and innate antitumor immunity, these changes may be related to systemic immunosuppression and inflammation to promote tumor progression in tumor-bearing mice. Moreover, MDSC accumulation and activation are driven by multiple secreted factors associated with chronic inflammation, including the cytokines, IL-1β and IL-6, leukotriene D4, prostaglandin E2, and inflammation-associated molecules, VEGF and GM-CSF [38].

This study confirmed that F3II tumor-bearing mice were susceptible to the engraftment of allogeneic MB16F10 tumors. As allogeneic tumor rejection is mediated by T cells [39], these results suggest that cellular immunity is compromised in mice bearing F3II tumors, where systemic immunosuppression enables tumors to evade host immunity. These results validate the findings reported in medical practice, where immunologists have noted that tumor-bearing patients are often immunosuppressed and unable to respond to their tumors, establishing tumor-induced immunosuppression as an important mechanism that enables the tumor to escape immune destruction [40]. This finding supports the involvement of systemic immunosuppression and explains the inability of the host to respond to pulmonary metastasis.

Established anticancer treatments utilize cytostatic drugs (chemotherapy), often in combination with surgical removal of primary solid tumors. Previous studies have described how resection of primary solid tumors reverses tumor-induced immunosuppression [39]. Here, we confirmed that surgery or high-dose doxorubicin and cyclophosphamide treatment significantly reduced F3II tumor-induced myeloid alterations, as shown by the return of the spleen and liver to their normal size. However, no changes were detected in the pulmonary metastases. One explanation for these observations could be that reducing the primary tumor burden decreases several immunosuppressive factors synthesized and secreted by tumor cells, thereby supporting immune recovery [39,41,42].

The primary result of this study indicated that F3II tumors mimic many characteristics of human breast cancer, specifically in relation to immune system effects. This murine model can provoke T cell exclusion and systemic immunosuppression linked to neutrophilia and thrombocytosis, as well as MDSC accumulation in the spleen, in addition to class I MHC overexpression and production of the pro-inflammatory cytokine, IL-6, by tumor cells. Additionally, the observed reversal in myeloid changes following tumor resection supports the hypothesis that neoplasia is the basis for the pathological changes detected in tumor-bearing mice.

These results support the occurrence of immune cell dysfunction mediated by the presence of F3II tumors in mice, which concurs with immune alterations characterized by chronic systemic

https://doi.org/10.4048/jbc.2022.25.e18

inflammation and immunosuppression described in breast cancer in a clinical setting. Thus, the F3II tumor model is a relevant model for evaluating novel breast cancer immunotherapies and their combinations in preclinical studies. Moreover, it can also be used for the identification of appropriate therapeutic targets and development of proof-of-concept experiments.

REFERENCES

1. Alonso DF, Farías EF, Urtreger A, Ladeda V, Vidal MC, Bal De Kier Joffé E. Characterization of F3II, a sarcomatoid mammary carcinoma cell line originated from a clonal subpopulation of a mouse adenocarcinoma. J Surg Oncol 1996;62:288-97.
PUBMED | CROSSREF
2. Fuentes D, Avellanet J, Garcia A, Iglesias N, Gabri MR, Alonso DF, et al. Combined therapeutic effect of a monoclonal anti-idiotype tumor vaccine against NeuGc-containing gangliosides with chemotherapy in a breast carcinoma model. Breast Cancer Res Treat 2010;120:379-89.
PUBMED | CROSSREF
3. Gabri MR, Menna PL, Scursoni AM, Gomez DE, Alonso DF. Role of tumor-derived granulocyte-macrophage colony-stimulating factor in mice bearing a highly invasive and metastatic mammary carcinoma. Pathobiology 1999;67:180-5.
PUBMED | CROSSREF
4. Katoh Y, Nakamura M, Ohnishi Y, Shimamura K, Ueyama Y, Tamaoki N. Autonomous production of granulocyte-colony stimulating factor in tumour xenografts associated with leukocytosis. Br J Cancer 1993;68:715-9.
PUBMED | CROSSREF
5. Datar I, Schalper KA. Epithelial-mesenchymal transition and immune evasion during lung cancer progression: the chicken or the egg? Clin Cancer Res 2016;22:3422-4.
PUBMED | CROSSREF
6. Lou Y, Diao L, Cuentas ER, Denning WL, Chen L, Fan YH, et al. Epithelial-mesenchymal transition is associated with a distinct tumor microenvironment including elevation of inflammatory signals and multiple immune checkpoints in lung adenocarcinoma. Clin Cancer Res 2016;22:3630-42.
PUBMED | CROSSREF
7. Schreiber RD, Old LJ, Smyth MJ. Cancer immunoediting: integrating immunity's roles in cancer suppression and promotion. Science 2011;331:1565-70.
PUBMED | CROSSREF
8. Joyce JA, Fearon DT. T cell exclusion, immune privilege, and the tumor microenvironment. Science 2015;348:74-80.
PUBMED | CROSSREF
9. Tumeh PC, Harview CL, Yearley JH, Shintaku IP, Taylor EJ, Robert L, et al. PD-1 blockade induces responses by inhibiting adaptive immune resistance. Nature 2014;515:568-71.
PUBMED | CROSSREF
10. Herbst RS, Soria JC, Kowanetz M, Fine GD, Hamid O, Gordon MS, et al. Predictive correlates of response to the anti-PD-L1 antibody MPDL3280A in cancer patients. Nature 2014;515:563-7.
PUBMED | CROSSREF
11. Diakos CI, Charles KA, McMillan DC, Clarke SJ. Cancer-related inflammation and treatment effectiveness. Lancet Oncol 2014;15:e493-503.
PUBMED | CROSSREF
12. Jiang S, Wang S, Wang Q, Deng C, Feng Y, Ma F, et al. Systemic inflammation response index (SIRI) independently predicts survival in advanced lung adenocarcinoma patients treated with first-generation EGFR-TKIs. Cancer Manag Res 2021;13:1315-22.
PUBMED | CROSSREF
13. Dolan RD, Lim J, McSorley ST, Horgan PG, McMillan DC. The role of the systemic inflammatory response in predicting outcomes in patients with operable cancer: systematic review and meta-analysis. Sci Rep 2017;7:16717.
PUBMED | CROSSREF
14. Armitage JD, Newnes HV, McDonnell A, Bosco A, Waithman J. Fine-tuning the tumour microenvironment: current perspectives on the mechanisms of tumour immunosuppression. Cells 2021;10:56.
PUBMED | CROSSREF

15. Mabuchi S, Sasano T, Komura N. Targeting myeloid-derived suppressor cells in ovarian cancer. Cells 2021;10:329.
PUBMED | CROSSREF

16. Yeo ECF, Brown MP, Gargett T, Ebert LM. The role of cytokines and chemokines in shaping the immune microenvironment of glioblastoma: implications for immunotherapy. Cells 2021;10:607.
PUBMED | CROSSREF

17. Ireson CR, Alavijeh MS, Palmer AM, Fowler ER, Jones HJ. The role of mouse tumour models in the discovery and development of anticancer drugs. Br J Cancer 2019;121:101-8.
PUBMED | CROSSREF

18. Pérez Sánchez L, Morera Díaz Y, Bequet-Romero M, Ramses Hernández G, Rodríguez Y, Castro Velazco J, et al. Experimental studies of a vaccine formulation of recombinant human VEGF antigen with aluminum phosphate. Hum Vaccin Immunother 2015;11:2030-7.
PUBMED | CROSSREF

19. Yang Y, Yang HH, Hu Y, Watson PH, Liu H, Geiger TR, et al. Immunocompetent mouse allograft models for development of therapies to target breast cancer metastasis. Oncotarget 2017;8:30621-43.
PUBMED | CROSSREF

20. Hanahan D, Weinberg RA. Hallmarks of cancer: the next generation. Cell 2011;144:646-74.
PUBMED | CROSSREF

21. Talmadge JE, Fidler IJ. AACR centennial series: the biology of cancer metastasis: historical perspective. Cancer Res 2010;70:5649-69.
PUBMED | CROSSREF

22. Morrison BJ, Steel JC, Morris JC. Reduction of MHC-I expression limits T-lymphocyte-mediated killing of cancer-initiating cells. BMC Cancer 2018;18:469.
PUBMED | CROSSREF

23. Aguilera TA, Giaccia AJ. Molecular pathways: oncologic pathways and their role in T-cell exclusion and immune evasion-a new role for the AXL receptor tyrosine kinase. Clin Cancer Res 2017;23:2928-33.
PUBMED | CROSSREF

24. Hegde PS, Karanikas V, Evers S. The where, the when, and the how of immune monitoring for cancer immunotherapies in the era of checkpoint inhibition. Clin Cancer Res 2016;22:1865-74.
PUBMED | CROSSREF

25. Grivennikov SI, Greten FR, Karin M. Immunity, inflammation, and cancer. Cell 2010;140:883-99.
PUBMED | CROSSREF

26. Mantovani A, Allavena P, Sica A, Balkwill F. Cancer-related inflammation. Nature 2008;454:436-44.
PUBMED | CROSSREF

27. Gay LJ, Felding-Habermann B. Contribution of platelets to tumour metastasis. Nat Rev Cancer 2011;11:123-34.
PUBMED | CROSSREF

28. Faria SS, Fernandes PC JrSilva MJ, Lima VC, Fontes W, Freitas-Junior R, et al. The neutrophil-to-lymphocyte ratio: a narrative review. Ecancermedicalscience 2016;10:702.
PUBMED | CROSSREF

29. Cao W, Yao X, Cen D, Zhi Y, Zhu N, Xu L. Prognostic role of pretreatment thrombocytosis on survival in patients with cervical cancer: a systematic review and meta-analysis. World J Surg Oncol 2019;17:132.
PUBMED | CROSSREF

30. Kim KM, Choi HS, Noh H, Cho IJ, Lim ST, Lee JI, et al. Neutrophil to lymphocyte ratio after treatment completion as a potential predictor of survival in patients with triple-negative breast cancer. J Breast Cancer 2021;24:443-54.
PUBMED | CROSSREF

31. Fridlender ZG, Sun J, Kim S, Kapoor V, Cheng G, Ling L, et al. Polarization of tumor-associated neutrophil phenotype by TGF-beta: "N1" versus "N2" TAN. Cancer Cell 2009;16:183-94.
PUBMED | CROSSREF

32. Keeley T, Costanzo-Garvey DL, Cook LM. Unmasking the many faces of tumor-associated neutrophils and macrophages: considerations for targeting innate immune cells in cancer. Trends Cancer 2019;5:789-98.
PUBMED | CROSSREF

33. Chechlinska M, Kowalewska M, Nowak R. Systemic inflammation as a confounding factor in cancer biomarker discovery and validation. Nat Rev Cancer 2010;10:2-3.
PUBMED | CROSSREF

34. Køstner AH, Nielsen PS, Georgsen JB, Parner ET, Nielsen MB, Kersten C, et al. Systemic inflammation associates with a myeloid inflamed tumor microenvironment in primary resected colon cancer-may cold tumors simply be too hot? Front Immunol 2021;12:716342.
PUBMED | CROSSREF

35. Lin RJ, Afshar-Kharghan V, Schafer AI. Paraneoplastic thrombocytosis: the secrets of tumor self-promotion. Blood 2014;124:184-7.
PUBMED | CROSSREF

36. Pietilä M, Ivaska J, Mani SA. Whom to blame for metastasis, the epithelial-mesenchymal transition or the tumor microenvironment? Cancer Lett 2016;380:359-68.
PUBMED | CROSSREF

37. Deng G. Tumor-infiltrating regulatory T cells: origins and features. Am J Clin Exp Immunol 2018;7:81-7.
PUBMED

38. Ostrand-Rosenberg S, Sinha P. Myeloid-derived suppressor cells: linking inflammation and cancer. J Immunol 2009;182:4499-506.
PUBMED | CROSSREF

39. Danna EA, Sinha P, Gilbert M, Clements VK, Pulaski BA, Ostrand-Rosenberg S. Surgical removal of primary tumor reverses tumor-induced immunosuppression despite the presence of metastatic disease. Cancer Res 2004;64:2205-11.
PUBMED | CROSSREF

40. Sakakura K, Chikamatsu K. Immune suppression and evasion in patients with head and neck cancer. Adv Cell Mol Otolaryngol 2013;1:21809.
CROSSREF

41. Predina JD, Kapoor V, Judy BF, Cheng G, Fridlender ZG, Albelda SM, et al. Cytoreduction surgery reduces systemic myeloid suppressor cell populations and restores intratumoral immunotherapy effectiveness. J Hematol Oncol 2012;5:34.
PUBMED | CROSSREF

42. Rashid OM, Nagahashi M, Ramachandran S, Graham L, Yamada A, Spiegel S, et al. Resection of the primary tumor improves survival in metastatic breast cancer by reducing overall tumor burden. Surgery 2013;153:771-8.
PUBMED | CROSSREF